

# Detailed Analysis of Coherence Collapse in Semiconductor Lasers

Hua Li, *Member, IEEE*, Jun Ye, and John G. McInerney, *Member, IEEE*

**Abstract**—Experimental and theoretical studies of coherence collapse in GaAs/AlGaAs laser diodes with weak optical feedback show two distinct routes to chaos. In each case we observe undamped relaxation oscillations, then external cavity mode beating, and finally coherence collapse. When there is frequency locking between the relaxation oscillations and external cavity modes, a period doubling sequence is followed, otherwise the route to chaos is via quasiperiodicity.

## I. INTRODUCTION

SEMICONDUCTOR lasers are extremely interesting as physical systems as well as very useful for engineering applications, and their dynamical properties have been studied intensively for several years. An especially important problem is the dynamics of these lasers when subject to external optical feedback. Optical feedback is highly effective in linewidth narrowing [1], [2] and mode selection [3], [4]. While single-mode diode lasers have free-running linewidths  $\sim 50$ – $100$  MHz at milliwatt output powers, use of relatively simple external cavities can reduce these linewidths to less than 1 MHz. Using anti-reflection coatings and grating external cavities can give linewidths as narrow as 10 kHz [5]. Optical feedback-induced dynamics can also occur inadvertently, and it is essential to allow for these effects in designing real systems [6], [7].

External cavity lasers are prone to exhibit various instabilities [8], of which the most common is coherence collapse, a sudden and catastrophic broadening of the linewidth to  $\sim 10$  GHz as the external cavity coupling (i.e., the degree of optical feedback) is increased [1], [9]–[14]. This occurrence is obviously deleterious for most practical applications, although it may actually be useful in suppressing coherent backscatter and speckle effects, for example in optical disk information storage. At high feedback levels ( $\sim 10\%$  in power) if the system is operated close to the kink found just below the isolated laser threshold, the laser is dominated by the external cavity, under these conditions there are several distinct and qual-

itatively different phenomena which could also legitimately be collectively described as coherence collapse, including subharmonic bifurcation [15], self-pulsation [16], intermittent behavior [17] and “staircase fluctuations” involving random power drops followed by stepwise recoveries [18], [19]. We shall use the term “coherence collapse” in this paper exclusively to describe the feedback-induced catastrophic line broadening in a single transverse and longitudinal mode semiconductor laser operating well above the isolated laser threshold (20–100%), when less than 0.1% of the output power is coupled back from a simple plane mirror located at  $\sim 10$  cm from the laser. Because of the minute amounts of feedback involved, there is no significant difference between the isolated and external cavity laser thresholds.

In this paper we present the results of detailed theoretical and experimental analyses whose primary purpose is to examine carefully the sequence of events which occurs as coherence collapse develops, to learn the underlying mechanisms, and to characterize the coherence-collapsed state. We are particularly interested in establishing beyond reasonable doubt whether coherence collapse is a stochastic or deterministic (chaotic) phenomenon. Although several authors have suggested that the coherence collapsed state is chaotic [10], [13], [14], the coherence collapsed semiconductor laser has been analyzed with some success by a variety of rate equation models including coherent feedback without noise [13], injection locking [20] and stochastic contributions [21]–[23]. Moreover, the issue has not been proven by calculation of characteristic dimensions [24] or other accepted means. Apart from its intrinsic theoretical significance, the answer to this question will determine how to eradicate or exploit coherence collapse. Section II describes our experimental results, while Section III describes our rate equation model. In Section IV we present experimental and theoretical results and make detailed comparisons between them. We also present the outcomes of calculations to determine the influence of noise on the coherence-collapsed state. Section V contains some discussion and conclusions.

## II. EXPERIMENTAL OBSERVATIONS

The experimental arrangement used (Fig. 1) was essentially identical to those employed in previous observations of coherence collapse: a GaAs/AlGaAs double-hetero-

Manuscript received July 30, 1992. This work was supported by the U.S. Air Force Office of Scientific Research, the U.S.A.F. Phillips Laboratory (PILOT program) and the Defense Advanced Research Projects Agency.

The authors are with the Optoelectronic Device Physics Group, Center for High Technology Materials, University of New Mexico, Albuquerque, NM 87131-6081.

J. G. McInerney is also with the Department of Physics, University College, Cork, Ireland.

IEEE Log Number 9211355.

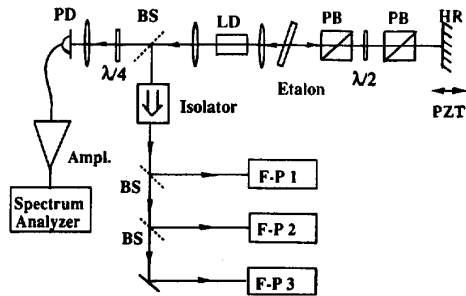


Fig. 1. Experiment arrangement.

junction laser diode (Hitachi HLP1400) with built-in lateral index guiding via the channeled substrate planar structure was placed in an external cavity formed by an antireflection-coated collimating lens and a high reflectivity plane mirror which reflected a portion of the output light back into the active region of the laser diode. The free-running laser diode oscillated in a single longitudinal and transverse mode at a wavelength close to 830 nm, although a tendency toward multiple diode mode operation was common under external feedback. No facet coatings were applied to the laser chip. A stabilized current source and temperature control were used to ensure intrinsic stability of the laser pumping: the absolute frequency drift was less than 100 MHz/min at all times during the experiments. The fraction of light coupled back into the laser was controlled by an attenuator consisting of a half-wave plate sandwiched between a pair of linear polarizers. A solid quartz etalon of free spectral range  $\sim 1$  THz and finesse  $\sim 30$  was inserted to force the laser to oscillate in a single longitudinal mode of the diode cavity (which contained many external cavity modes spaced by a frequency  $\nu_{\text{ext}}$ , close to  $c/2L_{\text{ext}}$ , where  $L_{\text{ext}}$  is the optical length of the external cavity). The bias current was set well above threshold, typically  $1.2\text{--}2.0 I_{\text{th}}$ . Thus the necessary conditions for coherence collapse were established.

To observe coherence collapse, the optical feedback was increased from zero, while intensity noise power spectra were measured using a fast p-i-n photodiode (Anatel AR-S2, 30 ps rise time) coupled to a microwave spectrum analyzer (Tektronix 2755P, 21 GHz bandwidth), and optical spectra were measured simultaneously using a suite of three scanning Fabry-Perot interferometers. Two of these instruments were plane-plane cavities, with free spectral ranges of 2150 GHz and 11 GHz and finesse  $> 100$ , enabling simultaneous observation of the overall laser diode mode spectrum (which remained single longitudinal mode throughout) and the fine side-band structures induced by the relaxation oscillation and external cavity modes. The third scanning Fabry-Perot was a confocal resonator with FSR 750 MHz and finesse 300, and was used to view narrowing of the laser linewidth at weak feedback levels.

It was not possible to record meaningful time series or accumulate sufficient data for experimental determination

of correlation dimensions or similar dynamical parameters: for this purpose, we would require both a fast sampling interval ( $\sim 10$  ps) and a large data set ( $\sim 10^5$  points) [35], a task which is beyond the limitations of currently available equipment.

Fig. 2 and Fig. 3 show the evolution of the laser dynamics with increasing optical feedback. In the absence of external feedback, the laser usually operated in a single longitudinal mode. The intensity noise power spectrum featured a small perturbation around the relaxation oscillation peak frequency  $\nu_R$ , indicating damped oscillation.  $\nu_R$  was easily identified by its strong dependence on the injection current. As the feedback was increased from zero, we initially observed linewidth narrowing, followed by the appearance of a sharp peak at  $\nu_R$  (or equivalently of sidebands situated a distance  $\nu_R$  on each side of the main peak in the optical spectrum). With further increase of the feedback fraction  $f_{\text{ext}}$  from the external mirror, we observed external cavity mode beating features spaced by  $\nu_{\text{ext}}$ : these were easily identified by their dependence on the cavity length. Nonlinear interaction occurred between the relaxation oscillation and external cavity mode beating with further increase in  $f_{\text{ext}}$  culminating in the irregular state known as coherence collapse. These data agree generally with the reported measurements of Dente *et al.* [13] and of Mørk *et al.* [14]. However, the details of this interaction differed according to whether there was an integer relation between the external cavity mode spacing  $\nu_{\text{ext}}$  and the relaxation oscillation resonance peak  $\nu_R$ .

Fig. 2 shows measured RF intensity power spectra in the usual situation where there is no integer ratio between  $\nu_{\text{ext}}$  and  $\nu_R$ ; the pump current is held constant ( $I/I_{\text{th}} = 1.59$ ) at fixed external cavity length (15.5 cm), while the feedback fraction  $f_{\text{ext}}$  from the external mirror was increased. The initial feedback-induced undamping of the relaxation oscillation and external cavity mode beating gives way to a complicated spectrum in which both the main laser oscillation peak and the relaxation oscillation sidebands are modulated by external cavity modes, with peaks at frequencies such as  $\nu_R - 6\nu_{\text{ext}}$  becoming evident. Here the interaction between  $\nu_{\text{ext}}$  and  $\nu_R$  is that of normal quasiperiodic mixing, and the coherence-collapsed state appears to be a chaotic one attained via a quasiperiodic route as surmised by Mørk *et al.* This conjecture will be examined further in Section IV.

Fig. 3 shows measured intensity noise and optical spectra as  $f_{\text{ext}}$  was increased but this time the external cavity mode spacing  $\nu_{\text{ext}}$  was held equal to an integer sub-multiple of the relaxation oscillation resonance peak  $\nu_R$  by judicious fine adjustments of the pump current and cavity length. (Here the current was nominally  $1.39 I_{\text{th}}$  while the external cavity length was 9.0 cm.) In this special case we observed peaks at  $\nu_{\text{ext}}$ ,  $\nu_{\text{ext}}/2$ ,  $\nu_{\text{ext}}/4$  appearing sequentially with increasing feedback, followed by the catastrophically broadened laser linewidth and broadband intensity noise spectrum characteristic of coherence collapse. Period-8 oscillations were observed only tentatively, probably due to the presence of noise and the lack

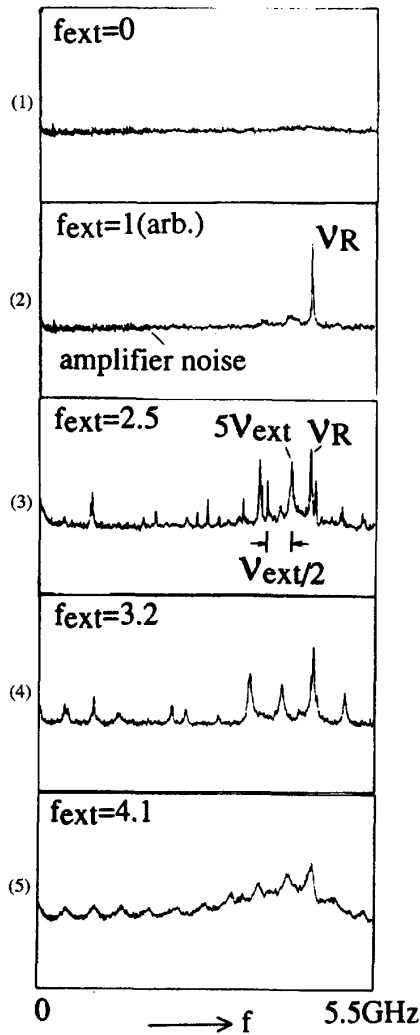


Fig. 2. Measured power spectra of intensity noise showing a quasiperiodic sequence to chaos.  $I/I_{th} = 1.59$ ,  $L_{ext} = 15.5$  cm.

of long-term stability in these experiments. The sidebands in the optical spectra are clearly asymmetric about the lasing frequency. From these results it is clear that the coherence collapsed state was reached via a period-doubling route, again suggesting the onset of deterministic chaos. This is the first observation of period doubling in an external cavity semiconductor laser and will be considered in detail in the next section.

In several long-term experiments on coherence collapse we observed predominantly the quasiperiodic route. The pure period-doubling route to chaos occurred only by careful selection of parameters. Although it was possible to observe period-doubling at fixed pump current and external cavity length, it was much more easily and clearly observed by fine-tuning the current or cavity length while increasing the feedback level. We also determined the usual quasiperiodic mixing process to be punctuated by regions of frequency locking between  $\nu_{ext}$  and  $\nu_R$ , al-

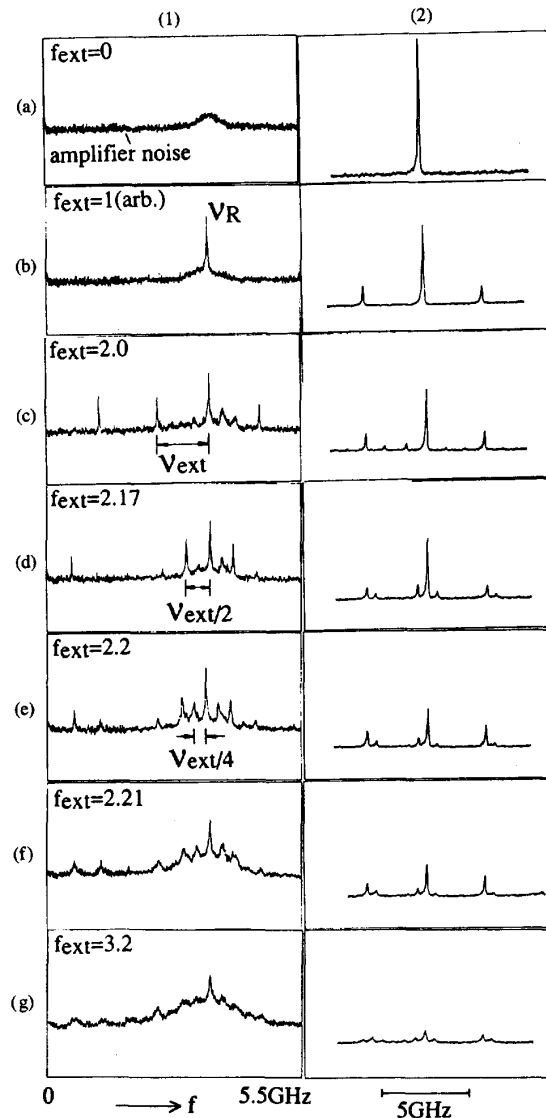


Fig. 3. Measured period-doubling sequence to chaos. (1) Power spectra of intensity noise; (2) Optical spectra.  $I/I_{th} = 1.38$ ,  $L_{ext} = 9$  cm.

though these regions were narrow and fragile and required careful observation. In the vicinity of these tentative frequency locking events, there was evidence of frequency pulling between  $\nu_{ext}$  and  $\nu_R$ .

One probable consequence of this behavior is the existence of hybrid processes involving mostly quasiperiodicity but including windows with weak frequency locking or pulling, sometimes a single period-doubling bifurcation. These effects were manifested by the appearance of peaks spaced by  $\nu_{ext}/2$  and  $\nu_{ext}/4$  at relatively high feedback levels close to coherence collapse. We also observed combination tones such as  $\nu_R - 6.5\nu_{ext}$  in the noise power spectrum (*cf.* Fig. 2), and again the process culminated in a seemingly chaotic coherence-collapsed state.

The external cavity length exerted a weak influence on

the qualitative nature of coherence collapse: the effect disappeared as  $L_{\text{ext}}$  is made very small. In general, for shorter external cavities (a few cm) the onset of coherence collapse occurred at higher feedback levels regardless of the particular route followed. In our experiments, when the cavity length was less than  $\sim 3$  cm, even with the maximum available feedback (i.e., the attenuator and the etalon removed from the external cavity) it was possible only to observe undamping of the relaxation oscillation; there was insufficient feedback to generate significant external cavity mode beating, and hence coherence collapse did not occur. When the external cavity length was increased to  $\sim 4$  cm, with maximum feedback we observed the undamped relaxation oscillation followed by emergence of the external cavity modes; in the absence of the intracavity etalon the system then tended toward mode hopping and multi-longitudinal mode operation, a tendency which increased with increasing cavity length. With the etalon in place, for cavity lengths from 6 cm to 50 cm, coherence collapse occurred in the same qualitative manner as described above, except that the feedback fraction  $f_{\text{ext}}$  at the onset of coherence collapse decreased as  $L_{\text{ext}}$  increased.

### III. THEORETICAL MODELING

We have adopted the usual rate equations for semiconductor lasers with the same modifications as other authors to allow for the weak optical feedback, and additionally taking into account the intraband relaxation of charge carriers and polarization within the conduction and valence bands via a finite saturation intensity for the laser gain per unit time

$$G = G_0 / (1 + I/I_s)^{1/2} \quad (1)$$

where  $I$  is the mode intensity in the laser resonator, and the saturation intensity  $I_s$  is related to the intraband relaxation times [26].  $G_0$  is the linear gain rate given as

$$G_0 = G_N(N - N_0) \quad (2)$$

where  $G_N$  is the differential gain,  $N$  is the carrier population and  $N_0$  is the value of  $N$  when the laser material is optically transparent. For a single mode isolated laser the rate equations have the following form [27], [28]

$$\frac{dI(t)}{dt} = \left[ \frac{G_N(N(t) - N_0)}{(1 + I(t)/I_s)^{1/2}} - \gamma_p \right] I(t) + R_{\text{sp}} + F_I(t) \quad (3)$$

$$\frac{d\Phi(t)}{dt} = \frac{\alpha}{2} [G_N(N(t) - N_0) - \gamma_p] + F_\Phi(t) \quad (4)$$

$$\frac{dN(t)}{dt} = J - \frac{N(t)}{\tau_s} - \left[ \frac{G_N(N(t) - N_0)}{(1 + I(t)/I_s)^{1/2}} \right] I(t) + F_N(t) \quad (5)$$

where  $\Phi$  is the phase of the field and  $\gamma_p$  is the resonator loss rate which is defined as:

$$\gamma_p = G_{\text{th}} = G_N(N_{\text{th}} - N_0) \quad (6)$$

$J$  is the pump rate,  $\tau_s$  is the carrier life time.  $R_{\text{sp}}$  is the spontaneous emission rate.  $\alpha$  is the antiguiding parameter or linewidth enhancement factor which governs the coupling between the optical intensity and phase in the laser: it is the ratio of the carrier-induced changes in the real and imaginary parts of the susceptibility [32], [33], and is customarily approximated by a constant in dealing with single mode laser dynamics.  $F_I(t)$ ,  $F_\Phi(t)$  and  $F_N(t)$  represent the Langevin forces of spontaneous emission noise for intensity, phase and carrier population, respectively.

It is clear that the optical phase is not coupled directly to the intensity  $I$  and carrier population  $N$ , so that the behavior of the isolated laser diode can be described completely by (3) and (5): the resulting two-dimensional space is insufficient to generate chaos. However, if we add optical feedback (or modulation, or light injection, or any of several other external stimuli) we have to expand the phase space, so the system can support many different rich dynamical phenomena. If the external cavity is weakly coupled so that it is sufficient to consider only one feedback delay term [29]–[31], the rate equations become:

$$\begin{aligned} \frac{dI(t)}{dt} = & \left[ \frac{G_N(N(t) - N_0)}{(1 + I(t)/I_s)^{1/2}} - \gamma_p \right] I(t) + R_{\text{sp}} \\ & + \kappa (I(t)I(t - \tau))^{1/2} \cos(\bar{\omega}\tau + \Phi(t) \\ & - \Phi(t - \tau)) + F_I(t) \end{aligned} \quad (7)$$

$$\begin{aligned} \frac{d\Phi(t)}{dt} = & \frac{\alpha}{2} [G_N(N(t) - N_0) - \gamma_p] - \kappa \left( \frac{I(t - \tau)}{I(t)} \right)^{1/2} \\ & \cdot \sin(\bar{\omega}\tau + \Phi(t) - \Phi(t - \tau)) + F_\Phi(t) \end{aligned} \quad (8)$$

$$\frac{dN(t)}{dt} = J - \frac{N(t)}{\tau_s} - \left[ \frac{N(t) - N_0}{(1 + I(t)/I_s)^{1/2}} \right] I(t) + F_N(t) \quad (9)$$

where  $\tau$  is the feedback delay (i.e., the round trip optical delay time in the external cavity),  $\bar{\omega}$  is the steady state laser frequency.  $\kappa$  is given as

$$\kappa = \frac{1 - R}{\tau_{LD} \sqrt{R}} (f_{\text{ext}})^{1/2} \quad (10)$$

where  $R$  is the facet reflectivity and  $\tau_{LD}$  is the optical round trip delay in the laser diode resonator and  $f_{\text{ext}}$  is the fraction of the laser output power coupled by the external cavity. Clearly we now have three coupled rate equations, the trajectory of the system is described in a three-dimensional phase space and deterministic chaos is now possible.

Equations (7)–(9) can be written in the general abbreviated form

$$\frac{d\vec{X}(t)}{dt} = f(\vec{X}(t)) + \kappa \cdot g(\vec{X}(t), \vec{X}(t - \tau)) + \vec{F}(t) \quad (11)$$

TABLE I  
LASER PARAMETERS USED IN CALCULATIONS

$G_N$	$5.3 \cdot 10^5/s$
$\gamma_p = G_{th}$	$5.8 \cdot 10^{11}/s$
$\tau_s$	$3.0 \cdot 10^{-9}/s$
$N_{th}$	$7.56 \cdot 10^8$
$N_0$	$6.45 \cdot 10^8$
$R_{sp}$	$1.5 \cdot 10^{12}/s$
$I_s$ (photons)	$5.0 \cdot 10^6$
$R$	0.32
$\tau_{LD}$	$7.5 \cdot 10^{-12}/s$
$\alpha$	5.3

where  $\vec{X}(t) = (I(t), \Phi(t), N(t))$ ,  $\vec{F}(t) = (F_I(t), F_\Phi(t), F_N(t))$  and  $f$  is a nonlinear function describing the isolated laser and  $\kappa \cdot g$  is the nonlinear feedback term with delay time  $\tau$  and strength  $\kappa$ . The field feedback parameter  $\kappa$  is uniquely specified by  $f_{ext}$ ,  $\tau_{LD}$  and  $R$  as described by (10).  $\vec{F}(t)$  is a Langevin force describing white noise driving. It is reasonable to take  $\kappa$  as a critical or control parameter in determining the dynamical behavior of the external cavity laser system; other parameters such as  $\tau$ ,  $I_s$ ,  $J$ , etc. will be assigned different values to assess their influences. In our theoretical modeling based on the above equations, we take all parameter values ( $R_{sp}$ ,  $G_N$ ,  $N_0$ ,  $N_{th}$ ,  $R$ , etc.) as close as possible to the values appropriate to the real GaAs/AlGaAs CSP single mode lasers used in the experiments (see Table I) [13], [27].

In our numerical modeling, we first calculated the time series of  $I(t)$ ,  $\Phi(t)$ ,  $N(t)$  by numerical integration of (7)–(9). The smallest time step in the integration was 7.5 ps which corresponded to a single round trip in the laser diode resonator. 70 000 data points were obtained and the first  $\sim 10$  000 points were discarded to avoid initial transients; hence approximately 60 000 data points remained to analyze the system dynamics over a total time interval of about 0.5  $\mu$ s. The corresponding Fourier frequency range was several tens of gigahertz which more than covered the bandwidth of the phenomena under study with a resolution  $\sim 2$  MHz.

Because the phase diffusion process causes difficulties in constructing trajectories in the phase space ( $I(t)$ ,  $\Phi(t)$ ,  $N(t)$ ), it was convenient to transform these phase  $\Phi(t)$  to the instantaneous deviation of the optical frequency from its steady state value using

$$\bar{\omega}(t) = \lim_{\delta t \rightarrow 0} \frac{\Phi(t) - \Phi(t - \delta t)}{\delta t} \quad (12)$$

and instead to construct trajectories in the modified phase space ( $I(t)$ ,  $\bar{\omega}(t)$ ,  $N(t)$ ). Thus the time series of these three variables, the corresponding intensity noise power spectra and autocorrelation function were calculated. In addition, bifurcation plots, Poincaré maps and correlation dimensions were obtained to provide further insights into the dynamics of the external cavity laser. The Langevin noise driving terms were switched on and off to determine the effects of realistic noise on the coherence collapse process.

## IV. RESULTS OF THEORETICAL SIMULATIONS

### A. Period Doubling

Initially we obtained stable steady state solutions by quenching the derivatives in the rate equations {(7)–(9)}, then used these steady state solutions as initial conditions for full numerical solutions of the time-dependent equations without noise terms. Where multiple stable steady state solutions existed, the one with the smallest frequency deviation from the isolated laser frequency was chosen. Because the most novel result of our experiment is the observation of a period-doubling bifurcation sequence to coherence collapse in a narrow parameter range, we checked a wide range of parameter values numerically to determine the regime in which period-doubling could be observed theoretically. Fig. 4 shows the results of these calculations: time series and noise power spectra of the intensity  $I(t)$ , with Poincaré maps and intensity autocorrelation functions. The Poincaré maps were plotted on the plane of constant carrier population  $N$ .

There is good agreement between theory and experiment. From Fig. 4 it is clear that as the feedback parameter  $\kappa$  increased, first the relaxation oscillation at frequency  $\nu_R$  was undamped, followed by excitation of the external cavity modes spaced by  $\nu_{ext}$ . When  $\nu_R$  was equal to an integer multiple of  $\nu_{ext}$ , period doubling was observed with fundamental period  $1/\nu_{ext}$ : the relaxation oscillation was initially modulated by  $\nu_{ext}$ , then by  $\nu_{ext}/2$  and  $\nu_{ext}/4$  sequentially. There is evidence of weak  $\nu_{ext}/8$  features in the power spectrum before the onset of coherence collapse with further increase in  $\kappa$  as shown in Fig. 4(E, G). Note also the existence of a window of regular oscillation (Fig. 4(F)) before full development of the coherence-collapsed state.

To examine this period-doubling behavior in more detail, we constructed a bifurcation plot corresponding to the calculations in Fig. 4. This was done by calculating the local peak values of the time series  $I(t)$  and hence the envelope of the relaxation for a given  $\kappa$ , then taking the local maxima of this envelope for this value of  $\kappa$ . The result is given as Fig. 5 in which the range of  $x$  covers the traces shown in Fig. 4. Again there is clear period doubling with fundamental period  $1/\nu_{ext}$ . We note that the values of the Feigenbaum universal constant  $\delta f$  and the relative scale of successive branch splittings  $\delta \epsilon$  in this bifurcation plot differ from the predicted values 4.6692  $\dots$  and 2.5029  $\dots$  [34], a result which is hardly surprising because  $\delta f$  and  $\delta \epsilon$  are defined in terms of the asymptotic behavior of the bifurcation splitting, whereas in our system the last observable bifurcation is only to period-4. Moreover, the external cavity laser under investigation is much more complicated than the usual systems undergoing period-doubling for which universality has been shown to be valid: apart from the main controllable feedback parameter  $\kappa$ , there are several other variables, such as the feedback delay time  $\tau$  and pump rate  $J$ , which also influence the real physical process.

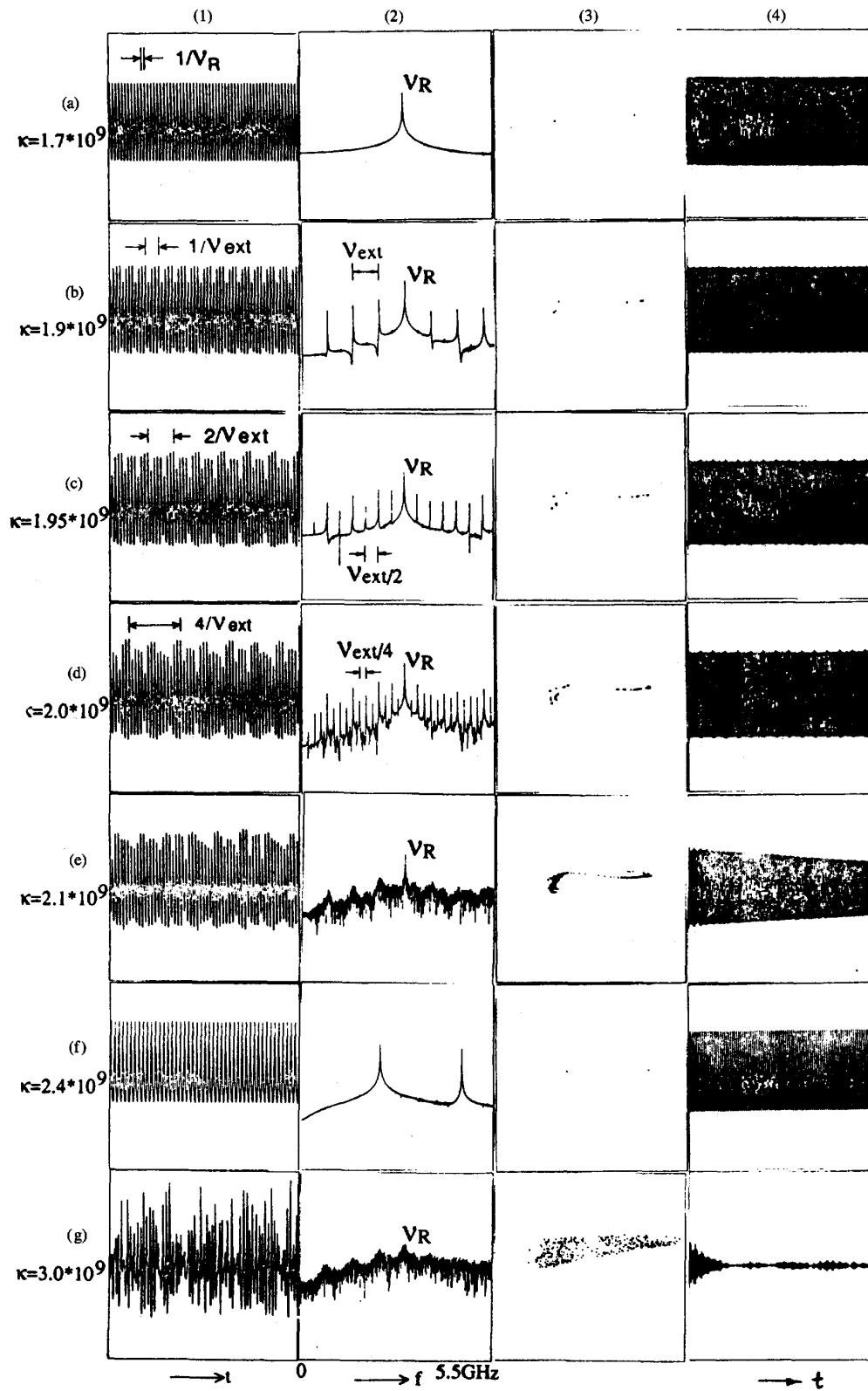


Fig. 4. Calculated period-doubling route to chaos as  $\kappa$  increased. (1) Time series of  $I(t)$ . (2) Power spectra of  $I(t)$ . (3) Poincaré maps for constant carrier population. (4) Autocorrelation function of  $I(t)$ .  $L_{ext} = 18$  cm;  $\alpha = 5.3$ ;  $I_s = 5.0 \times 10^6$  (photons);  $J = 3.25 \times 10^{17}$  /s (corresponding  $I/I_{th} \approx 1.5$ ).

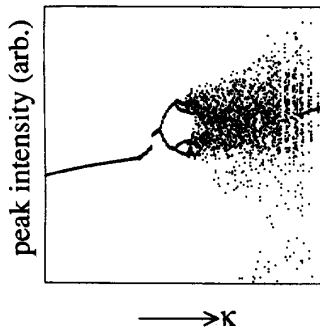


Fig. 5. Bifurcation plot showing the period-doubling sequence of Fig. 4.

### B. Dimensionality Analysis of the Coherence-Collapsed State

Our experiments and theory have demonstrated clearly the existence of period-doubling bifurcation and aperiodic behavior in coherence collapse. However, the conclusion that coherence collapse in this system is deterministic chaos which occurs through period-doubling has not been justified until a clear distinction is made between chaos and random noise. Strange or chaotic attractors are typically characterized by fractal dimensions  $D_2$  which are smaller than the number of degrees of freedom [32], hence we expect a strange attractor in our three-dimensional phase space to show a fractal dimension between 2 and 3, in contrast to a purely stochastic process which fills the whole phase space and hence has dimension 3.

To clarify the essential nature of the coherence collapsed state, we have performed a dimensionality test on our theoretical data, and the results are given in Fig. 6, in which the letters A–F again indicate the data in Fig. 4. The calculation of the correlation dimension  $D_2$  was performed in the real phase space ( $I(t)$ ,  $\omega(t)$ ,  $N(t)$ ) using conventional box counting techniques [24], [36]. Referring to Fig. 6, the trajectory is initially a limit cycle (dimension unity) corresponding to undamped simple relaxation oscillation, progressing to a chaotic attractor with a fractal dimension between 2 and 3 as coherence collapse develops. We note that the correlation dimension  $D_2$  is a function of the feedback parameter  $\kappa$ ;  $D_2$  in the coherence-collapsed state for finite  $\kappa$  is always less than 3, and it tends to 3 as  $\kappa$  tends to infinity. The regular oscillation window is consistently indicated by  $D_2 = 1$ . These data provide clear evidence that the onset of coherence collapse by period doubling is deterministic chaos but not a stochastic process. The role of realistic noise in this picture will be considered later.

Considerable effort has been devoted to choosing the correct structure of the data set and comparing different techniques in determining the value of  $D_2$ . The greatest difficulty is encountered in determining  $D_2$  just as the system approaches coherence collapse (point E in Figs. 4–6): the intensity autocorrelation function here decays slowly compared with the fastest time constant of the system (i.e., the relaxation oscillation period) so that the

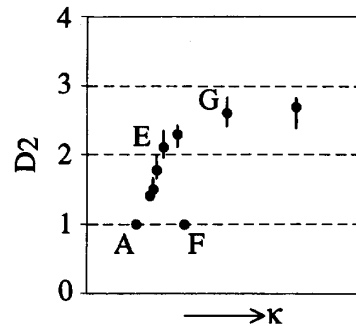


Fig. 6. Calculated dimension  $D_2$  corresponding to the sequence of Fig. 4.

problem is stiff and large data sets must be used. To alleviate the logistical problems in this analysis, for this case we initially calculated  $D_2$  using all points in very large data sets ( $\sim 130\,000$  points after truncation of initial transients) using a supercomputer, then compared the results with calculations using  $\sim 60\,000$  points, and found no significant difference. However, obvious differences were seen using  $\sim 40\,000$  points. To choose the best technique for calculating  $D_2$  we compared different methods such as single variable embedding techniques using the definitions of Grassberger *et al.* [36]–[38], finding pointwise dimensions in a real phase space at different points [39], and evaluating correlation dimensions in a real phase space with direct box counting techniques [24]. Nonuniform attractor densities cause undulations in the log-log plots of the correlation integral  $C(r)$  versus box size  $r$  which make the slopes of these plots uncertain, resulting in errors in the  $D_2$  values, whichever technique was used. We ultimately selected averaging of the pointwise dimension at 100 randomly chosen points from the trajectory, an approach which provided good results with minimal computation times. Thus most of the  $D_2$  values were then obtained using this simplified technique and with  $\sim 60\,000$  data points.

Although the pure period-doubling route to chaos occurred only within a narrow parametric range, frequency components involving  $\nu_{\text{ext}}/2$  and  $\nu_{\text{ext}}/4$  could also appear in the quasiperiodic route. Again we emphasize that a properly scaled sequence of period doubling bifurcations from the fundamental period  $1/\nu_{\text{ext}}$  is what distinguishes the alternative route to coherence collapse. Since a symmetric system cannot undergo period doubling [40], we postulate that in the external cavity laser the effects of external feedback are different for the two sidebands of the lasing mode (due to dispersion as expressed by the antiguiding or linewidth enhancement factor  $\alpha$ ). Thus the optical feedback causes symmetry breaking and that makes period doubling possible. In contrast, period-doubling from the relaxation oscillation period  $T_R = 1/\nu_R$  has never been observed in the external cavity laser.

### C. Quasiperiodic Route to Coherence Collapse

Similar calculations were performed for the situation corresponding to the experimental data in Fig. 2, in which

a quasiperiodic route to coherence collapse was observed when the frequency locking condition  $\nu_R = p\nu_{\text{ext}}$  (integer  $p$ ) was not satisfied. Again there is very good agreement as illustrated by Fig. 7 where calculated intensity noise power spectra and Poincaré maps are plotted for increasing optical feedback. Fig. 8 shows a bifurcation plot obtained in a similar manner to Fig. 5, and the calculated correlation dimension versus feedback parameter  $\kappa$  is given in Fig. 9.

As  $\kappa$  increases, first the relaxation oscillation is excited (Fig. 7B), then the external cavity mode features appear, modulating both the main lasing peak and the relaxation oscillation sidebands. Quasiperiodic mixing occurs as evidenced by difference frequencies such as  $\nu_R - 6\nu_{\text{ext}}$  and  $7\nu_{\text{ext}} - \nu_R$ , and with further increase in  $\kappa$  there are traces of features spaced by  $\nu_{\text{ext}}/2$  and possibly even  $\nu_{\text{ext}}/4$ , resulting in frequency components such as  $\nu_R - 6.5\nu_{\text{ext}}$ . Despite the occurrence of  $\nu_{\text{ext}}/2$  and  $\nu_{\text{ext}}/4$  in the noise spectra this is not a period doubling scenario, but typical quasiperiodic behavior involving mixing of frequencies which are not commensurate or rationally related. The correlation dimension plot again shows that the coherence collapsed state is chaotic, with a similar  $D_2$  value (a fractal between 2 and 3) to the result of the period doubling sequence observed when frequency locking was maintained between  $\nu_R$  and  $\nu_{\text{ext}}$ . In the experiments, the maximum broadened linewidth in the coherence collapsed state (refer to Fig. 2 and Fig. 3) was  $\sim 30\text{--}40$  GHz which corresponded to the bandwidth of the isolated laser resonator. Beyond this effective bandwidth limit of the system the external cavity modes as well as the relaxation oscillation harmonics are strongly suppressed.

Just as in the experiments, coherence collapse usually occurs in the theoretical model via a quasiperiodic route. Even when period doubling does occur, it is not robust: small changes in the external cavity length  $L_{\text{ext}}$  ( $\sim \lambda/4$ ) or the drive current (less than 0.1%) can destroy the frequency locking condition and produce a quasiperiodic route to chaos. Also, we have observed situations where frequency locking conditions are satisfied at low feedback, but as  $\kappa$  increases the locking condition is violated and the onset of coherence collapse proceeds via the more usual quasiperiodic route.

#### D. Influence of Spontaneous Emission Noise

The influence of spontaneous emission noise on the dynamics of the external cavity semiconductor laser has been studied theoretically by switching on realistic Langevin forces  $F_I(t)$ ,  $F_\Phi(t)$ ,  $F_N(t)$  representing white noise driving on the right side of the rate equations  $\{(7)\text{--}(9)\}$ . In the numerical integration of these equations the method in [41] was used to generate Gaussian noise.

Fig. 10 shows the influence of realistic white noise on the intensity noise power spectra and phase space trajectories for the case where frequency locking occurred and the trajectory was a limit cycle. Although the white noise driving caused noisy pedestals in the intensity noise spec-

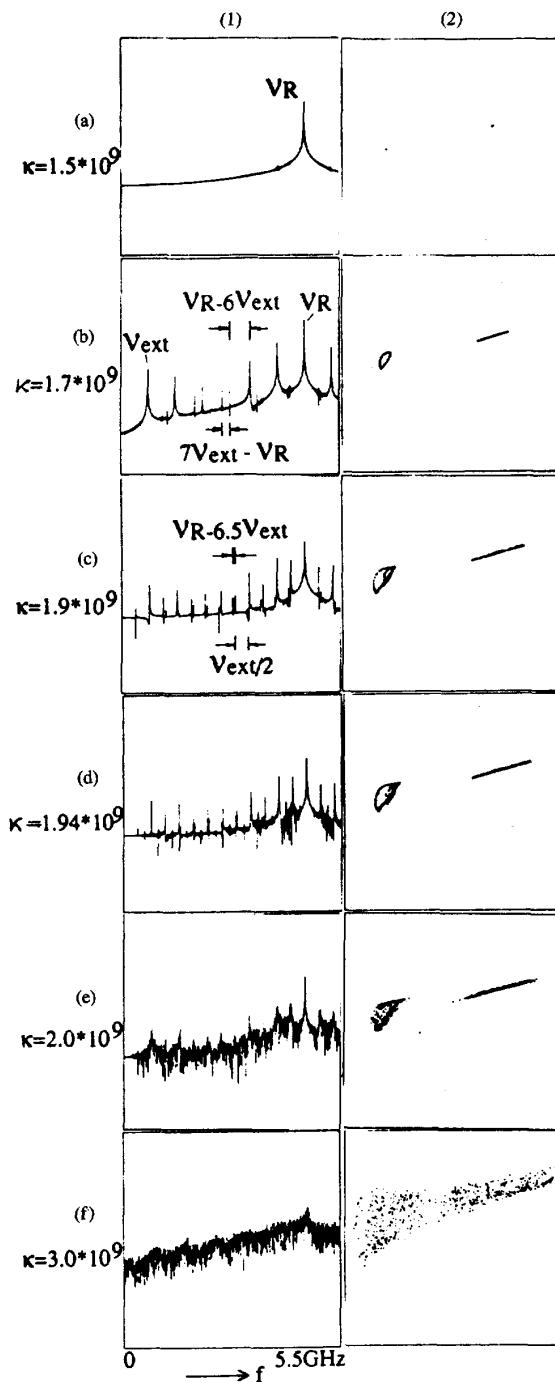


Fig. 7. Calculated power spectra of intensity noise and Poincaré map showing quasiperiodic route to chaos.  $L_{\text{ext}} = 18$  cm,  $\alpha = 4$ ,  $I_s = 5.0 \cdot 10^7$  (photons),  $J = 4.2 \cdot 10^{17}$  /s (corresponding  $I/I_{\text{th}} \cong 1.68$ ).

tra and blurred the trajectories in phase space, the essential features of the attractor were not altered. As the spontaneous emission rate  $R_{\text{sp}}$  increased, the noise intensity increased and the external cavity modes became weaker. Fig. 11 gives the corresponding calculations of the cor-

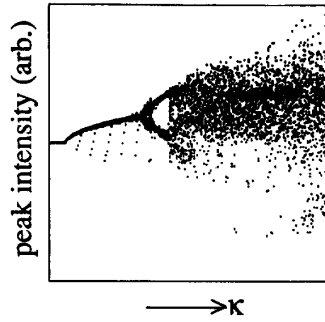


Fig. 8. Bifurcation plot showing the quasiperiodic sequence of Fig. 7.

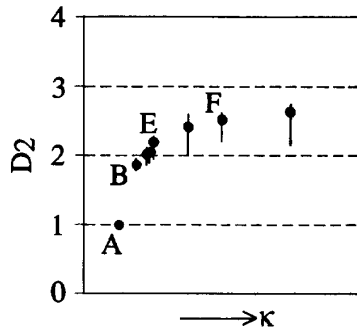


Fig. 9. Calculated dimension  $D_2$  for the sequence of Fig. 7.

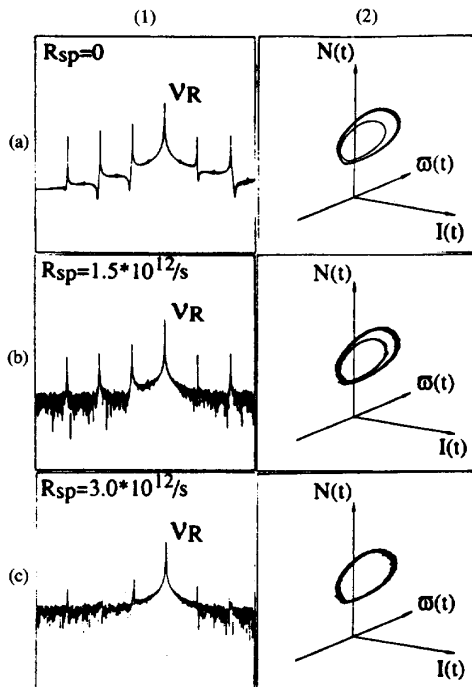


Fig. 10. Calculated power spectra of intensity noise and trajectories with-out and with white noise driving at different levels.  $L_{ext} = 18$  cm,  $\alpha = 5.3$ ,  $I_s = 5.0 \times 10^6$  (photons),  $J = 3.25 \times 10^{17}$ /s,  $\kappa = 1.9 \times 10^9$ .

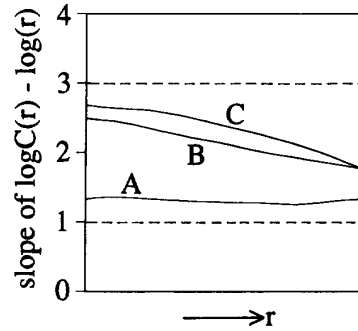


Fig. 11. Calculated slope of log-log plots of the correlation integral vs. box size  $r$ . The parameters are the same as those used in Fig. 10. (1)  $R_{sp} = 0$ ; (2)  $R_{sp} = 1.5 \times 10^{12}$ /s; (3)  $R_{sp} = 3.0 \times 10^{12}$ /s.

relation dimension showing that the slopes  $S(r)$  of the log-log plots of the correlation integral versus box size  $r$  decreased monotonically with  $r$  as white noise driving was added, a fact which makes it difficult to determine  $D_2$  in real experimental situations. As the box size  $r$  decreased,  $S(r)$  increased and tended toward 3, indicating that the noise was filling the phase space and dominating the dynamics when we examined only a very small domain in the phase space.

Fig. 12 shows the influence of realistic white noise on a chaotic coherence collapsed state. Again the noise driving did not change the intensity noise spectra very much, but blurred the phase space trajectories. The corresponding correlation dimension calculations in Fig. 13 are very similar to those in Fig. 11 in that the dimension with noise driving tended toward 3 as the box size  $r$  approached zero, and it was always larger than that without noise driving. However, the  $D_2$  value for the coherence-collapsed state never reached 3—coherence collapse was always attributable to deterministic chaos. We also performed dimensional calculations for the isolated laser with realistic white noise, and the convergent  $D_2$  value was always 3 within a small computational error. This value was never exceeded by the maximum value of  $S(r)$  in a feedback system with noise driving, hence we conclude that white noise driving does not change the deterministic nature of the system.

In our stochastic calculations the value of the spontaneous emission rate  $R_{sp}$  was taken as  $1.5 \times 10^{12}$ /s and  $3.0 \times 10^{12}$ /s. The value of  $R = 1.5 \times 10^{12}$ /s led to a calculated Lorentzian linewidth of about 40 MHz in the isolated laser diode at pump current  $I/I_{th} = 1.68$ , in agreement with experimental measurements. The spectral density of the noise was assumed white, and no attempt was made to include “natural” low-frequency noise with a  $1/f$  spectral dependence.

Figs. 11 and 13 show that with noise driving  $S(r)$  did not converge. This difficulty is generic to all real systems involving a mixture of deterministic and stochastic processes where the definitions of characteristic dimensions may not be meaningful. It is sufficient here that we have found that deterministic processes are the dominant influ-

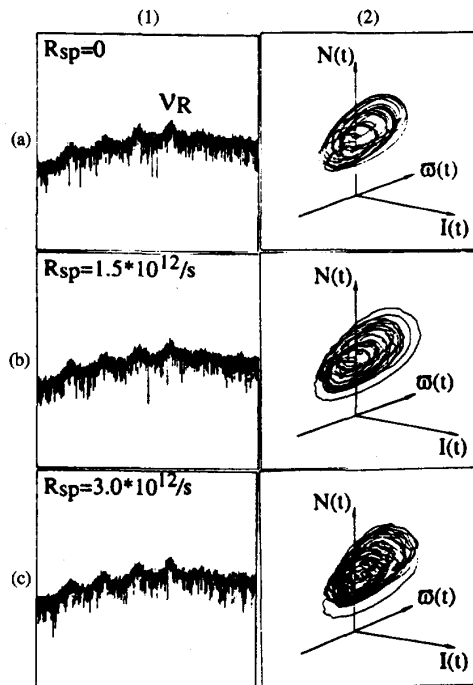


Fig. 12. Calculated power spectra of intensity noise and trajectories with-out and with white noise driving at different levels.  $L_{\text{ext}} = 18$  cm,  $\alpha = 5.3$ ,  $I_s = 5.0 \times 10^6$  (photons),  $J = 3.25 \times 10^{17}$ /s,  $\kappa = 3.0 \times 10^9$ .

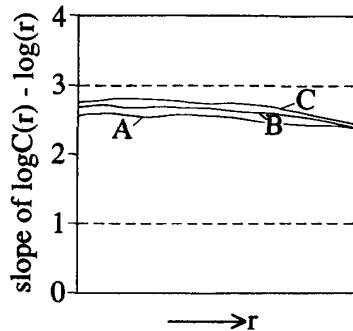


Fig. 13. Calculated slope of log-log plots of the correlation integral vs. box size  $r$ . The parameters are same as those used in Fig. 12. (1)  $R_{\text{sp}} = 0$ ; (2)  $R_{\text{sp}} = 1.5 \times 10^{12}$ /s; (3)  $R_{\text{sp}} = 3.0 \times 10^{12}$ /s.

ences in coherence collapse, despite the very high spontaneous emission rates in semiconductor lasers, larger by several orders of magnitude than in other laser systems.

## V. DISCUSSION AND CONCLUSIONS

We have shown experimentally and theoretically the progression of events leading to coherence collapse in a semiconductor laser subject to weak optical feedback ( $\sim 0.01$ – $0.1\%$  in power) from a simple reflector several centimeters away. The laser was operated well above

threshold ( $1.2$ – $2.0 I_{\text{th}}$ ) and was constrained to operate in a single longitudinal mode of the diode cavity. As the feedback level increased, the laser initially underwent linewidth narrowing, then undamping of the relaxation oscillations, excitation of external cavity modes, and finally reached the coherence-collapsed state through one of two different routes or occasionally by a hybrid between them. A period-doubling route to chaos occurred only when the relaxation oscillation and external cavity modes or their harmonics were locked together, otherwise a quasiperiodic route was followed. In each case the proximate cause of coherence collapse was interaction between the feedback-induced undamped relaxation oscillation and the external cavity modes. We obtained excellent agreement between theory and experiment. From theoretical calculations of the correlation dimensions we showed that the coherence-collapsed state is a chaotic attractor with a fractal dimension between 2 and 3, even with the inclusion of realistic spontaneous emission noise.

Chaos occurred most frequently via quasiperiodicity, since frequency locking did not usually occur. When frequency locking did occur, it could be destroyed by small perturbations to the pump current or external cavity length. Most incidents of coherence collapse should therefore be due to quasiperiodic mixing between the relaxation oscillation and external cavity modes. The onset of coherence collapse occurred (for a given pump current and cavity length) at a certain value of the feedback parameter  $\kappa$  and did not depend on the particular route (period-doubling or quasiperiodicity).

At higher pump currents it is more difficult to produce coherence collapse when there is significant gain saturation or suppression, for example due to intraband scattering in the semiconductor. We attribute this to saturation-induced damping of the relaxation oscillation, which makes it more difficult to generate undamped relaxation oscillation, a necessary precursor to coherence collapse in our case.

Lasers with optical feedback are good examples of the generic nonlinear system with delayed feedback which has already been studied [42], [43]. In the external cavity laser the optical feedback effectively modulates the gain and constrains the optical phase, and the system formally becomes infinite-dimensional by considering each external cavity mode to be a separate degree of freedom. Even with the limited bandwidth of the system the effective dimension is still very large and the problem is not tractable. Here we have adopted the more straightforward alternative of considering the total laser intensity and phase (i.e., the sum of all the modes) to be single degrees of freedom while allowing sufficient time and bandwidth to include all the mode dynamics in the picture, thus effectively reducing the problem to three dimensions.

Our results could be generalized for a greater understanding of laser instabilities. The semiconductor laser is a typical class B laser:  $\gamma_p, \gamma_1 \ll \gamma_2$ , where  $\gamma_p, \gamma_1$  and  $\gamma_2$  are the decay rates of the photons, injected minority carriers (i.e., population inversion) and polarization, respec-

tively. Thus the free-running semiconductor laser is well described by rate equations with only two independent variables, usually the photon and carrier numbers or densities. The dynamical properties of isolated semiconductor lasers are therefore relatively simple. However, when an additional degree of freedom is added such as pump current modulation, optical feedback, external light injection, mutual coupling to another laser etc., the situation becomes much more complicated. The deterministic instabilities in this case are always connected with the interaction between some external modulation (external cavity modes in our case) and undamped intrinsic oscillations (relaxation oscillation in our case). We suggest that this behavior may be common to several laser systems under different circumstances, and it may be a very general scenario for an externally modulated Class B laser. For example, similar phenomena have been observed in single mode CO<sub>2</sub> lasers (which are also typical Class B lasers) with modulated cavity *Q*-factors, and these phenomena have also been explained in terms of interaction between the modulation and relaxation oscillation [44]. There are also interesting comparisons to be developed with multimode laser dynamics, where generally similar behavior—period-doubling and quasiperiodic routes to deterministic chaos—has been discovered [45]–[48]. Those lasers (and several other physical systems) may have intrinsic natural frequencies for oscillations. These oscillations are normally damped out but may be excited by external perturbations which are either external modulations or beatings between unequally spaced longitudinal or transverse modes. These excited intrinsic oscillations will then tend to interact with external modulations due to nonlinearities in the laser medium. Thus the study of coherence collapse may lead to extensive physical insights into nonlinear dynamics and chaos in lasers and similar physical systems well beyond the usual limitations of the simple rate equation theories used.

#### ACKNOWLEDGMENT

The authors express gratitude to N. B. Abraham for helpful discussion.

#### REFERENCES

- [1] L. Goldberg, H. F. Taylor, A. Dandridge, J. F. Weller, and R. O. Miles. "Spectral characteristics of semiconductor lasers with optical feedback," *IEEE J. Quantum Electron.*, vol. QE-18, pp. 555–564, Apr. 1982.
- [2] E. Patzak, H. Olesen, A. Sugimura, S. Saito, and T. Mukai. "Spectral linewidth reduction in semiconductor lasers by an external cavity with weak optical feedback," *Electron. Lett.*, vol. 19, pp. 938–940, Oct. 1983.
- [3] M. W. Fleming and A. Mooradian. "Spectral characteristics of external-cavity controlled semiconductor lasers," *IEEE J. Quantum Electron.*, vol. QE-17, pp. 44–59, Jan. 1981.
- [4] M. B. Snipes and J. G. McInerney. "Transverse mode filtering of wide stripe semiconductor lasers using an external cavity," *SPIE Proc.*, vol. 1634, Laser Diode Technology and Applications IV, pp. 542–551, 1992.
- [5] R. Wyatt and W. J. Devlin. "10 kHz linewidth 1.5  $\mu\text{m}$  InGaAsP external cavity laser with 55 nm tuning range," *Electron. Lett.*, vol. 19, pp. 110–112, Feb. 1983.
- [6] T. Morikawa, Y. Mitsuhashi, and J. Shimada. "Return-beam induced oscillations in self-coupled semiconductor lasers," *Electron. Lett.*, vol. 12, pp. 435–436, Aug. 1976.
- [7] Ch. Risch, and C. Voumard. "Self-pulsation in the output intensity and spectrum of GaAs-AlGaAs CW diode lasers coupled to a frequency-selective external optical cavity," *J. Appl. Phys.*, vol. 48, pp. 2083–2085, May 1977.
- [8] K. Otsuka. "Nonlinear phenomena in semiconductor lasers," *SPIE Proc.*, vol. 1497, Nonlinear Optics and Materials, pp. 432–443, 1991.
- [9] R. O. Miles, A. Dandridge, A. B. Tveten, H. F. Taylor, and T. G. Giallorenzi. "Feedback-induced line broadening in CW channel-substrate planar laser diodes," *Appl. Phys. Lett.*, vol. 37, pp. 990–992, Dec. 1980.
- [10] D. Lenstra, B. H. Verbeek, and A. J. den Boef. "Coherence collapse in single-mode semiconductor lasers due to optical feedback," *IEEE J. Quantum Electron.*, vol. QE-21, pp. 674–679, June 1985.
- [11] H. Olesen, J. H. Osmundsen, and B. Tromborg. "Nonlinear dynamics and spectral behavior for an external cavity laser," *IEEE J. Quantum Electron.*, vol. QE-22, pp. 762–773, June 1986.
- [12] R. W. Tkach and A. R. Chraplyvy. "Regimes of feedback effects in 1.5- $\mu\text{m}$  distributed feedback lasers," *J. Lightwave Technol.*, vol. LT-4, pp. 1655–1661, Nov. 1986.
- [13] G. C. Dente, P. S. Durkin, K. A. Wilson, and C. E. Moeller. "Chaos in the coherence collapse of semiconductor lasers," *IEEE J. Quantum Electron.*, vol. 24, pp. 2441–2447, Dec. 1988.
- [14] J. Mørk, J. Mark, and B. Tromborg. "Route to chaos and competition between relaxation oscillations for a semiconductor laser with optical feedback," *Phys. Rev. Lett.*, vol. 65, pp. 1999–2002, Oct. 1990.
- [15] T. Mukai and K. Otsuka. "New route to optical chaos: successive-subharmonic-oscillation cascade in a semiconductor laser coupled to an external cavity," *Phys. Rev. Lett.*, vol. 55, pp. 1711–1714, Oct. 1985.
- [16] J.-D. Park, D.-S. Soe, and J. G. McInerney. "Self-pulsations in strongly coupled asymmetric external cavity semiconductor lasers," *IEEE J. Quantum Electron.*, vol. 26, pp. 1353–1362, Aug. 1990.
- [17] J. Sacher, W. Elsaesser, and E. O. Goebel. "Intermittency in the coherence collapse of a semiconductor laser with external feedback," *Phys. Rev. Lett.*, vol. 63, pp. 2224–2227, Nov. 1989.
- [18] H. Temkin, N. A. Olsson, J. H. Abeles, R. A. Logan, and M. B. Panish. "Reflection noise in index-guided InGaAsP Lasers," *IEEE J. Quantum Electron.*, vol. QE-22, pp. 286–293, Feb. 1986.
- [19] C. H. Henry and R. F. Kazarinov. "Instability of semiconductor lasers due to optical feedback from distant reflectors," *IEEE J. Quantum Electron.*, vol. QE-22, pp. 294–301, Feb. 1986.
- [20] B. Tromborg and J. Mørk. "Nonlinear injection locking dynamics and the onset of coherence collapse in external cavity lasers," *IEEE J. Quantum Electron.*, vol. 26, pp. 642–654, Apr. 1990.
- [21] N. Schunk and K. Peterman. "Numerical analysis of the feedback regimes for a single-mode semiconductor laser with external feedback," *IEEE J. Quantum Electron.*, vol. QE-24, pp. 1242–1247, July 1988.
- [22] J. S. Cohen and D. Lenstra. "Spectral properties of the coherence collapsed state of a semiconductor laser with delayed optical feedback," *IEEE J. Quantum Electron.*, vol. QE-25, pp. 1143–1151, June 1989.
- [23] J. Wang and K. Peterman. "Noise analysis of semiconductor lasers within the coherence collapse regime," *IEEE J. Quantum Electron.*, vol. 27, pp. 3–9, Jan. 1991.
- [24] P. Grassberger and I. Procaccia. "Measuring the strangeness of strange attractors," *Physica 9D*, pp. 189–208, 1983.
- [25] A. Ben-Mizrachi, I. Procaccia, and P. Grassberger. "Characterization of experimental (noisy) strange attractors," *Phys. Rev. A*, vol. 29, pp. 975–977, Feb. 1984.
- [26] G. P. Agrawal. "Effect of gain and index nonlinearities on single-mode dynamics in semiconductor lasers," *IEEE J. Quantum Electron.*, vol. 26, pp. 1901–1909, Nov. 1990.
- [27] C. H. Henry. "Theory of the phase noise power spectrum of a single mode injection laser," *IEEE J. Quantum Electron.*, vol. QE-19, pp. 1391–1397, Sept. 1983.
- [28] G. P. Agrawal and N. K. Dutta. "Long-Wavelength Semiconductor Laser," Van Nostrand Reinhold Company, New York, 1986.
- [29] R. Lang and K. Kobayashi. "External optical feedback effects on semiconductor injection laser properties," *IEEE J. Quantum Electron.*, vol. QE-16, pp. 347–355, Mar. 1980.
- [30] R.-Q. Hui and S.-P. Tao. "Improved rate equations for external cavity semiconductor lasers," *IEEE J. Quantum Electron.*, vol. QE-25, pp. 1580–1584, June 1989.

- [31] D.-S. Seo, J.-D. Park, J. G. McInerney, and M. Osinski. "Multiple feedback effect in asymmetric external cavity semiconductor lasers," *IEEE J. Quantum Electron.*, vol. 25, pp. 2229-2238, Nov. 1989.
- [32] C. H. Henry. "Theory of linewidth of semiconductor lasers," *IEEE J. Quantum Electron.*, vol. QE-18, pp. 259-264, Feb. 1982.
- [33] M. Osinski and J. Buus. "Linewidth broadening factor in semiconductor lasers—an overview," *IEEE J. Quantum Electron.*, vol. QE-23, pp. 9-29, Jan. 1987.
- [34] H. G. Schuster. "Deterministic Chaos," *VCH Verlagsgesellschaft*, Weinheim, 1988.
- [35] L. M. Narducci, E. J. Quil, and J. R. Tredicci. "Laser and Quantum Optics," *World Scientific*, pp. 186-194, 1988.
- [36] P. Grassberger and I. Procaccia. "Estimation of the kolmogorov entropy from a chaotic signal," *Phys. Rev. A*, vol. 28, pp. 2591-2593, Oct. 1983.
- [37] A. M. Albano, J. Muench, C. Schwarz, A. I. Mees, and P. E. Rapp. "Singular-value decomposition and the Grassberger-Procaccia algorithm," *Phys. Rev. A*, vol. 38, pp. 3017-3026, Sept. 1988.
- [38] A. I. Mees, P. E. Rapp, and J. S. Jennings. "Singular-value decomposition and embedding dimension," *Phys. Rev. A*, vol. 36, pp. 340-346, July 1987.
- [39] J. D. Farmer, E. Ott, and J. A. Yorke. "The dimension of chaotic attractors," *Physica 7D*, pp. 153-180, 1983.
- [40] J. W. Swift and K. Wiesenfeld. "Suppression of period doubling in symmetric system," *Phys. Rev. Lett.*, vol. 52, pp. 705-708, Feb. 1984.
- [41] R. X. Fox, I. R. Gatland, R. Roy, and G. Vemuri. "Fast, accurate algorithm for numerical simulation of exponentially correlated colored noise," *Phys. Rev. A*, vol. 38, pp. 5938-5940, Dec. 1988.
- [42] K. Ikeda and K. Kondo. "Successive higher-harmonic bifurcations in systems with delayed feedback," *Phys. Rev. Lett.*, vol. 49, pp. 1467-1470, Nov. 1982.
- [43] B. Dorizzi, B. Grammaticos, M. Le Berre, Y. Pomeau, E. Ressayre, and A. Tallet. "Statistics and dimension of chaos in differential delay systems," *Phys. Rev. A*, vol. 35, pp. 328-339, Jan. 1987.
- [44] J. R. Tredicce, F. T. Arecchi, G. P. Puccioni, A. Poggi, and W. Gadomski. "Dynamics behavior and onset of low-dimensional chaos in a modulated homogeneously broadened single-mode laser: experiments and theory," *Phys. Rev. A*, vol. 34, pp. 2073-2081, Sept. 1986.
- [45] W. Klische and C. O. Weiss. "Instabilities and routes to chaos in a homogeneously broadened one- and two-mode ring laser," *Phys. Rev. A*, vol. 31, pp. 4049-4041, June 1985.
- [46] D. J. Biswas and R. G. Harrison. "Experimental evidence of three-mode quasiperiodicity and chaos in a single longitudinal, multi-transverse-mode cw CO<sub>2</sub> laser," *Phys. Rev. A*, vol. 32, pp. 3835-3837, Dec. 1985.
- [47] L. M. Hoffer, T. H. Chyba, and N. B. Abraham. "Spontaneous pulsing, period doubling, and quasiperiodicity in a unidirectional, single-mode, inhomogeneously broadened ring laser," *J. Opt. Soc. Am. B*, vol. 2, pp. 102-107, Jan. 1985.
- [48] C. O. Weiss. "Observation of instabilities and chaos in optically pumped far-infrared lasers," *J. Opt. Soc. Am. B*, vol. 2, pp. 137-140, Jan. 1985.

**Hua Li** (M'93), photograph and biography not available at the time of publication.

**Jun Ye**, photograph and biography not available at the time of publication.

**John G. McInerney** (M'81), photograph and biography not available at the time of publication.